Critical density fluctuations in lipid bilayers detected by fluorescence lifetime heterogeneity

Anthony Ruggiero and Bruce Hudson
Department of Chemistry, Molecular Biology Institute and Chemical Physics Institute, University of Oregon, Eugene, Oregon 97403

ABSTRACT The heterogeneity of the decay of the fluorescence of *trans*-parinaric acid in single-component lipid bilayers at temperatures above their gel/liquid crystalline phase transition is shown to be due to the presence of regions of higher local density and higher acyl chain order than the predominant fluid regions. This conclusion is based on selective excitation behavior and the observation of time-resolved fluorescence anisotropies that increase at long times. The fractional amplitude of the long lifetime component of the fluorescence shows a temperature variation that conforms to conventional descriptions of critical behavior. The critical exponent extracted from this variation is 1.1, close to the value of 1.0 that describes ultrasonic data. We therefore conclude that liquid crystalline lipid bilayers exhibit critical behavior with significant density and order fluctuations. This behavior must be taken into account in the interpretation of fluorescence and other spectroscopic measurements of the properties of bilayers.

INTRODUCTION

Lipid bilayers are of fundamental importance both as models of biological membranes and intrinsically as lyotropic liquid crystals. Over the years, the physical properties of these systems have been extensively studied by a variety of experimental and theoretical techniques. It is well known that aqueous dispersions of phospholipid bilayers undergo a thermally induced order-disorder phase transition in which the lipid acyl chains change from a predominantly all-*trans* configuration in the "gel" phase to a disordered rotational isomeric state involving several gauche bonds in the "liquid crystalline" phase. An accurate experimental description of this transition on the molecular level is essential to the development and testing of molecular theories that explicitly confront the statistical mechanical details of the interparticle forces and correlations that determine the macroscopic physical properties of these systems. Any attempt to understand the more complex biological systems and the effects of various membrane additives such as cholesterol, proteins, antibiotics, or anesthetics on a microscopic level must be based on a detailed understanding of the structure and phase behavior of pure, single-component lipid systems.

Lipid bilayers also provide challenging systems for the interpretation of experiments because reorientational motion is locally anisotropic. The analysis of results for these systems is often dependent on models whose choice is influenced by the investigator's picture of bilayer chain order, dynamics, and phase behavior. This picture is influenced by the time scale of the measurements and on the extent to which they measure local or global properties. An important aspect of this interpretation is the extent to which the bilayer may be viewed as a uniform homogeneous structure.

Although the lipid bilayer phase transition has received considerable attention (Nagle, 1980; Lee, 1977), the exact nature of the transition, as well as the microscopic details, are not well understood. This ambiguity stems primarily from the fact that the lipid phase transition exhibits both first- and second-order characteristics (Nagle, 1973 *a* and *b*, 1976; Nagle and Scott, 1978; Mouritsen et al., 1983; Mouritsen and Zuckerman, 1985; Mitaku et al., 1978, 1981, 1982, 1983; Jahnig, 1981*a–c*). Whereas abrupt changes are seen in some physical properties, indicating a first-order transition, other properties display continuous changes and pretransitional behavior characteristic of second-order behavior. As the transition temperature is approached from above, for instance, response functions such as the ultrasonic velocity (Mitaku et al., 1978, 1981, 1982, 1983), passive permeability (Papahadjopoulos et al., 1973; Doniach, 1978; Nagle and Scott, 1978) and the specific heat as shown recently by ac calorimetry (Hatta et al., 1983, 1984), all begin to diverge. Before divergence actually occurs, however, this behavior is interrupted by a first order phase change. Whereas pretransitional phenomena are not usually observed in the properties of simple systems undergoing first-order phase transitions, this type of "weak" first order transition is quite common in isotropic to nematic transitions and transitions between different mesophases of liquid crystals (Priestley et al., 1975; Stinson and Litster, 1970; deGennes, 1972, 1974). The pseudocritical behavior of response functions in these systems is attrib-

0006-3495/89/06/1111/14 $2.00

uted to the presence of enhanced fluctuations of local order in the disordered bulk material as the transition temperature is approached. If a small region of the material in the disordered phase rearranges into a locally ordered structure as a result of a spontaneous fluctuation, the system will generally have an enhanced response to an external stimulus. The corresponding response function will therefore increase in magnitude. If the fluctuations occur to a very great extent (as they do when a second order transition is approached), then the response functions begin to diverge. The increased probability of thermodynamic fluctuations in liquid crystal systems, and the associated pretransitional phenomena, can be attributed to the smaller entropy change associated with these transitions compared with the entropy change of a melting/freezing transition in a simple liquid (Wojtowicz, 1975).

The similarities between the transition properties of lipid bilayers and nematic liquid crystals suggest that pretransitional fluctuations may also play an important role in the lipid "gel" to "liquid crystalline" transition. Density measurements (Nagle, 1973; Nagle and Wilkinson, 1978) and ultrasonic studies (Mitaku et al., 1982) on single-component lipid bilayer vesicles support this view and provide evidence for the existence of long-range structural fluctuations in the vicinity of the phase transition point. The fluctuations detected by ultrasonic measurements have a relaxation time on the tens of nanosecond time scale and a temperature dependence characteristic of critical phenomena. The magnitude of the ultrasonic relaxation time and strength, along with the critical exponents calculated for these quantities, agree well with those values obtained for the liquid crystal isotropic to nematic transition (Mitaku et al., 1983). Recent Monte Carlo treatments of models of the lipid bilayer phase transition by Mouritsen and Zuckerman (1983, 1985) have demonstrated the importance of the inclusion of density fluctuations in these models. The existence of long-lived metastable cluster states and slow relaxation behavior was shown by Mouritsen and Zuckerman (1985) to be caused by the presence of intermediate lipid chain conformational states that can kinetically stabilize the cluster distributions. As noted by these authors, the importance of spatially highly nonuniform configurations and fluctuations to the thermodynamics of lipid bilayer models implies that mean-field descriptions of the phase transition, despite their success in interpreting bilayer thermal behavior (McCammon and Deutch, 1975; Schindler and Seelig, 1975; Jacobs et al., 1975; 1977; Marcelja, 1976; Marcelja and Wolfe, 1979; Berde et al., 1980), are oversimplifications. It has been emphasized by Nagle that this critical behavior is expected for the bilayer transition because of the importance of the excluded volume effect in determining the order-disorder transition of these systems (Nagle, 1973*a* and *b*, 1976).

Whereas these and other theoretical studies (Jahnig, 1981*a–c*; Zuckermann and Pink, 1980; Kanehisa and Tsong, 1978) indicate that the coexistence and dynamical fluctuation of ordered and disordered phases should play an important role in the lipid bilayer phase transition, actual experimental evidence for this behavior has been limited primarily to measurements of the anomalous behavior of macroscopic response functions near the transition point. Direct experimental observation of microscopic cluster formation or the dynamic coexistence of lipid structural domains is complicated by the relative timescales of the experimental technique and the relaxation time of the fluctuations. Methods that average over timescales longer than the characteristic relaxation time of the domains will show only average behavior. In addition, the cooperative nature of the phenomena make it difficult to observe by techniques such as NMR, ESR, or fluorescence that reflect the mobility and interactions associated with both the internal molecular geometry and short range intermolecular forces between a probe molecule and the surrounding bulk. Despite these experimental difficulties, the sensitivity and time resolution of the fluorescence technique can, in principle, be used to detect coexisting regions of different lipid structure. What is needed is a fluorescence probe species whose spectral properties depend on the structural differences between the coexisting regions.

The presence and nature of fluctuations in bilayer density and acyl chain order, and the dynamics of the dissipation of these fluctuations, is important in several respects. Ultimately this critical behavior relates to the nature of the structure of the bilayer and the possibilities for organization of the environment of important functional components of membranes (Owicki et al., 1978). It has been suggested on the basis of Landau-type theories of bilayers that proteins, cholesterol, and other components of bilayers enhance the second-order nature of the phase transition at the expense of the first-order transition behavior (Jahnig, 1981*a–c*; Schroder, 1977). This suggestion relates to the interpretation of multicomponent systems in terms of critical fluctuations rather than phase equilibria (Mitaku and Okano, 1981; Sakanishi et al., 1979; Knoll et al., 1983). The construction of a successful theoretical treatment of a bilayer is strongly influenced by the extent to which long-range, long-lived fluctuations are important. This is most easily seen from consideration of a simulation of a bilayer by a molecular dynamics calculation (Kox et al., 1980; Busico and Vacatello, 1983; van der Ploeg and Berendsen, 1982, 1983; Northrup and Curvin, 1985). The degree of importance of cooperative behavior determines the minimum size and

trajectory time that must be used in such simulations. As noted, the interpretation of many experiments is also influenced by the spatial extent and time scale of these fluctuations. Measurements that reflect short-time, local behavior will detect heterogeneity that does not exist for longer-time scale, global measurements. Conflicting interpretations can result. A more speculative aspect of the importance of critical behavior involves the degree to which changes in the local structure of a membrane can influence the structure at a distant point. In a model where long-range order is important, structural changes can propagate cooperatively without lateral diffusion.

Ultrasonic relaxation measurements performed as a function of frequency and temperature (Mitaku et al., 1978, 1983; Mitaku and Date, 1982; Mitaku and Okano, 1981) provide evidence that the critical density fluctuations present in bilayers at temperatures just above T_m have a persistence time as long as 50 ns. Fluorescence lifetimes are typically on the order of a few nanoseconds and thus it may seem surprising that such variations in lateral density and (presumably) orientational order have not been previously detected in fluorescence experiments. If these density fluctuation regions represent a significant fraction of the bilayer, then their presence has to be considered in the interpretation of fluorescence experiments that might otherwise appear to be anomalous. The lack of emphasis on this instantaneous heterogeneity of the bilayer in the interpretation of fluorescence experiments may reflect the lack of sensitivity of many commonly used probe species to variation in the density of the local hydrocarbon environment.

The potential use of time-resolved fluorescence measurements for the detection of bilayer heterogeneity has been previously discussed (Barrow and Lentz, 1985) and has been applied to situations in which it is thermodynamically favorable for the lipid bilayer to be in a two-phase state (Klausner et al., 1980; Karnovski et al., 1982). In the present work a detailed analysis of the complex fluorescence decay behavior and time-resolved polarization anisotropy of the fluorescent fatty acid probe, *trans*-parinaric acid (*all trans*-9,11,13,15-octadecatetraenoic acid), is used to provide direct experimental evidence on the microscopic level for the existence of "solidlike" lipid domains in single-component fluid phase bilayer vesicles at temperatures slightly above that of their gel-to-liquid crystalline phase transition. The relaxation time of these domains is comparable to or longer than the fluorescence lifetime of this probe. This critical behavior is revealed by nonexponential fluorescence decay of the probe species, the observation of selective fluorescence excitation of the components, and characteristically different reorientational freedom of motion for each microenvironment. These properties demonstrate the presence of regions with a higher lateral density and higher acyl chain order compared with the bulk of the bilayer liquid crystalline phase. The detection of this heterogeneity is possible because of the particular properties of parinaric acid, especially the sensitivity of its absorption spectrum and fluorescence lifetime to local density. The interpretation of these properties is possible because of the extensive characterization of this probe, its known orientation in the lipid bilayer and the relative similarity of this species to normal acyl chain components of the bilayer (Sklar et al., 1975, 1976, 1977*a* and *b*; Wolber and Hudson, 1981; Hudson and Cavalier, 1988).

MATERIALS AND METHODS

L-α-Dipalmitoylphosphatidylcholine (DPPC), L-α-dielaidoylphosphatidylcholine (DEPC) and L-α-dioleoylphosphatidylcholine (DOPC) were used as purchased (Sigma Chemical Co., St. Louis, MO) and stored in the dark at −20°C. All lipids were pure as judged by thin layer chromatography and free of fluorescent impurities in the wavelength region of interest. *Trans*-parinaric acid was prepared by published methods (Sklar et al., 1977*a*; Wolber, 1980) and stored in degassed ethanol under argon in black taped containers at −20°C. The *trans*-parinaric acid was judged to be pure by both absorption and emission spectroscopy. Phosphate buffer (100 mM potassium phosphate) was prepared in the pH range 7.0–7.5 from reagent grade materials, degassed by repeated freeze-pump-thaw cycles, and stored under argon at 4°C before use.

Unilamellar vesicles were prepared from 30 mg/ml ethanolic solutions of phosphatidylcholine by the ethanol injection technique of Kremer et al. (1977). Residual ethanol was allowed to leak from the vesicles by holding them at the lipid-transition temperature for ~15 min and then annealing 10–15°C above the transition temperatures for an additionl 15 minutes. Vesicles prepared in this manner are 80–100 nm in diameter as observed in negative stained electron micrographs and exhibit the same 1–2°C phase transition width (as detected by *trans*-parinaric acid fluorescence intensity) observed for multilamellar vesicles (Wolber and Hudson, 1981). These vesicles do not undergo aggregation or fusion under the conditions of these experiments (Williamson et al., 1983). Lipid dispersions were labeled with *trans*-parinaric acid by addition of an aliquot of a concentrated ethanolic solution at a temperature above the lipid phase transition point. All samples were prepared and handled in a nitrogen-filled glove bag and then sealed under argon in fluorescence cuvettes. Oxygen-free samples prepared in this manner showed no signs of photodegradation or impurity fluorescence under the experimental conditions. Typical fluorescence samples contained 0.3 mg/ml of lipid with lipid-to-probe molar ratios of 200:1–400:1.

Fluorescence experiments were performed using time-correlated single photon counting (Philips, 1985; Demas, 1983; Fleming, 1986). A schematic diagram of the apparatus is shown in Fig. 1. The excitation source was a cavity-dumped rhodamine 6G dye laser (Spectra-Physics Inc., Mountain View, CA) synchronously pumped by a mode-locked Spectra-Physics CW Nd:YAG laser. The dye laser was cavity dumped at 800 kHz. At this pulse repetition rate the single-pulse autocorrelation traces were on the order of 10 ps (FWHM). The dye laser output near 600 nm was frequency doubled by type I angle-tuned phase matching in KDP (potassium dihydrogen phosphate) to provide UV excitation between 280 and 320 nm. The KDP crystal was mounted in a specially

designed cell filled with index matching fluid within which it could be rotated. The fluid index matched the second harmonic wavelength to the crystal and prevented beam displacement as the crystal was tuned by changing the angle. To prevent the fundamental beam from moving, it was separated from the harmonic beam with a dichroic beamsplitter, folded with a prism, and passed a second time through the crystal. This optical arrangement permits both the dye laser frequency and the crystal phase matching angle to be tuned without movement of the second harmonic beam at the sample or the fundamental wavelength beam at the photodiode.

The samples were excited through a calcite Glan-Thompson polarizer with vertically polarized light. Emission was collected at right angles to the excitation after passing through a Polaroid HNP'B polarizer oriented with its transmission axis either parallel, perpendicular, or at the magic angle (54.7°) relative to the excitation polarization depending on whether a fluorescence anisotropy or lifetime measurement was being

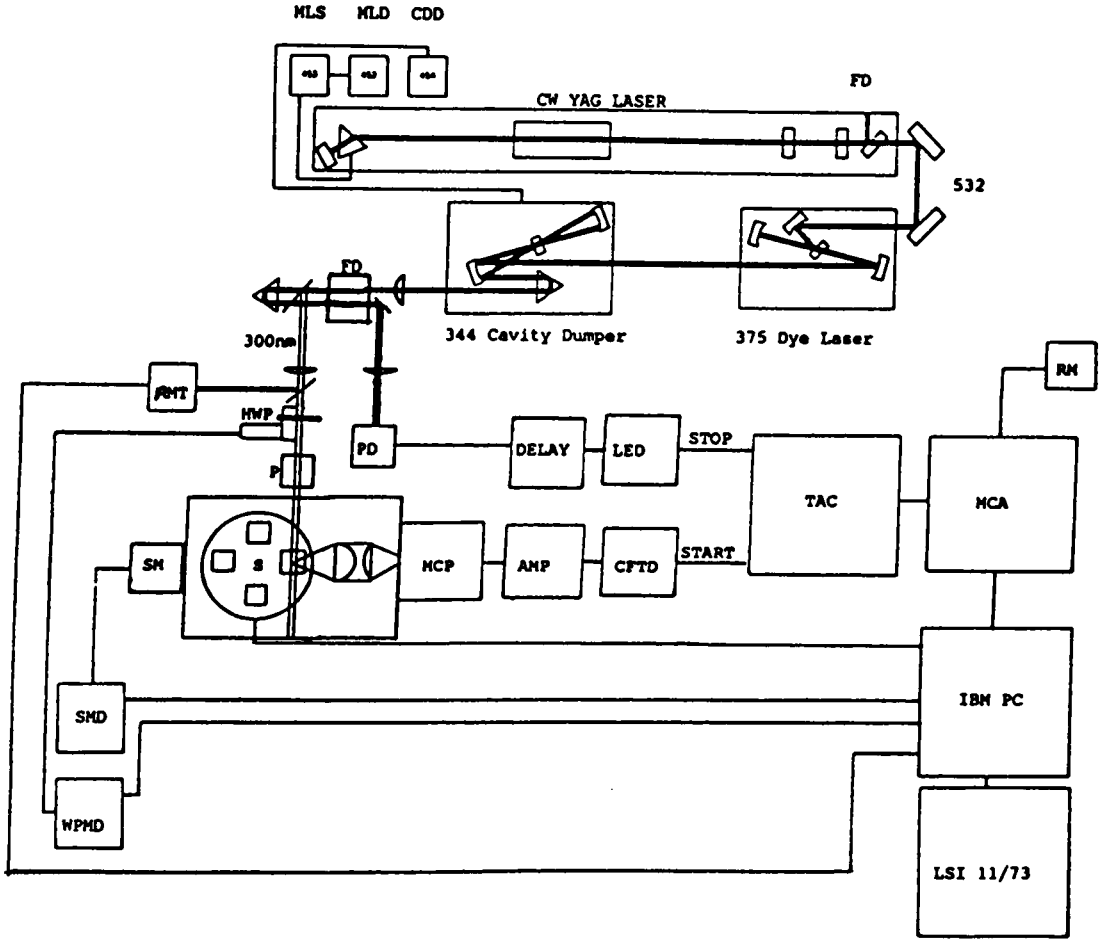

FIGURE 1 A schematic illustration of the single-photon counting apparatus used for these experiments. A mode-locked cw Nd:YAG laser (*top*) produces 7 W of average power at 1,064 nm. This is converted to 700 mW of average power at 532 nm using a potassium titanyl phosphate (KTP) cyrstal. The width of the mode-locked pulses is ~90 ps. A cavity-dumped jet stream dye laser is synchronously pumped with the 532 nm radiation. The resulting radiation near 600 nm has a pulse width of ~1 ps and a repetition rate of dc to 4 MHz. This radiation is converted to the ultraviolet by doubling with a potassium dideuterophosphate (KD*P) crystal. The resulting 300 nm radiation is directed to the sample. The residual 600 nm radiation is directed to a high-speed photodiode to produce a timing stop pulse. (This is optically isolated from the rest of the electronics to prevent spurious signals.) The arrival of a photon at the sample microchannel plate detector initiates a start pulse. A small amount of the 300 nm radiation is sampled by a photomultiplier to monitor the laser intensity. For anisotropy experiments the data is collected for constant integrated ilumination intensity. The beam intensity can also be adjusted by a halfwave plate polarization rotator. The UV light is polarized before being absorbed by the sample. The four-chamber rotating stage sample holder is temperature-controlled by a thermoelectric heater/cooler. It can operate well below 0°C when cooled with chilled water or refrigered ethylene glycol. The output of a time-to-amplitude converter is stored in a Tracor-Northern multichannel analyzer. This is repetitively dumped to an IBM-PC for data storage. A frequency counter provides a display of the data acquisition rate. The data from the IBM-PC is transferred to a DEC LSI 11/73 for analysis, plotting, etc. Figure labels: MLS, modelocker stabilizer; MLD, modelocker driver; CDD, cavity dumper driver; FD, frequency doubler; PMT, photomultiplier tube; PD, photodiode; HWP, ½ waveplate rotator; WPMD, ½ waveplate motor driver; P, polarizer; SM, sample stage motor; SMD, stage motor driver; MCP, microchannel plate photomultiplier; AMP, amplifier; CFTD, constant fraction timing discriminator; LED, leading edge timing discriminator; TAC, time-to-amplitude converter; RM, ratemeter; MCA, multichannel analyzer; PC, personal computer; DEC LSI 11/73, computer.

made. Scattered laser light was removed from the fluorescence with model 5-59 broadband blue transmission (Corning Glass Works, Corning, NY) and model WG-360 long-pass cut-off filters (Schott Glass Technologies Inc., Duryea, PA). In some cases, 10-nm-wide band pass interference filters were used to resolve the emission spectrum. The fluorescence was detected by a model R1294U electrostatically focused microchannel plate photomultiplier (MCP-PMT) (Hamamatsu Corp., Middlesex, NJ) operated at 3,000 V. Anode signals from the MCP were amplified with a model 8447D 1 GHZ preamplifier (Hewlett-Packard Co., Palo Alto, CA) and then discriminated with a model 934 quad constant fraction discriminator (CFTD) (EG&G Ortec, Oak Ridge, TN) to produce a timing signal. The CFTD output provided the "start" pulse for an Ortec 457 time-to-amplitude converter (TAC). The "stop" pulse was obtained by monitoring the dye laser fundamental with a 403B high-speed photodiode (Spectra-Physics Inc.). The output of the photodiode was discriminated with an Ortec 436 leading edge discriminator and delayed with an Ortec 425D nanosecond delay and a suitable length of 50 ohm coaxial cable as judged appropriate for a given TAC

Table 1 Fluorescence decay component analysis for *trans*-parinaric acid in DEPC bilayer vesicles at 15°C as a function of excitation wavelength

EX	T	Anal	α_1	τ_1	α_2	τ_2	α_3	τ_3	χ^2
nm	°C								
290	15	LSQ	0.363	40.850	0.145	2.157	0.492	7.272	1.034
			(0.022)	(2.521)	(0.034)	(0.365)	(0.018)	(0.634)	
290	15	MOMCE	0.369	40.000	0.136	2.038	0.494	7.122	
290	15	MOMS	0.358	41.357	0.147	2.091	0.494	7.358	
295	15	LSQ	0.351	39.587	0.145	1.770	0.504	6.902	1.060
			(0.015)	(1.704)	(0.020)	(0.239)	(0.011)	(0.388)	
295	15	MOMCE	0.352	40.000	0.139	1.945	0.508	6.993	
295	15	MOMS	0.349	39.170	0.147	1.514	0.503	6.747	
300	15	LSQ	0.243	40.156	0.292	3.364	0.465	7.689	1.363
			(0.032)	(4.683)	(0.114)	(0.511)	(0.085)	(1.342)	
300	15	MOMCE	0.247	40.000	0.219	2.999	0.532	7.168	
300	15	MOMS	0.261	36.023	0.150	1.511	0.588	6.159	
302	15	LSQ	0.328	38.846	0.165	2.626	0.507	7.067	1.114
			(0.021)	(2.380)	(0.057)	(0.478)	(0.040)	(0.710)	
302	15	MOMCE	0.317	40.000	0.165	2.472	0.517	7.152	
302	15	MOMS	0.353	36.525	0.094	2.197	0.552	6.370	
305	15	LSQ	0.358	39.304	0.218	3.437	0.424	7.764	1.015
			(0.002)	(2.000)	(0.048)	(0.376)	(0.047)	(0.414)	
305	15	MOMCE	0.350	40.000	0.246	3.587	0.402	8.196	
305	15	MOMS	0.397	35.470	0.089	2.144	0.513	6.229	
310	15	LSQ	0.361	39.304	0.162	2.694	0.477	7.421	1.121
			(0.002)	(2.000)	(0.024)	(0.293)	(0.024)	(0.228)	
310	15	MOMCE	0.348	40.000	0.159	2.148	0.492	7.420	
310	15	MOMS	0.386	40.983	0.166	2.212	0.493	7.604	
312	15	LSQ	0.306	39.304	0.256	3.396	0.438	7.990	1.456
			(0.002)	(2.000)	(0.042)	(0.296)	(0.042)	(0.390)	
312	15	MOMCE	0.299	40.000	0.221	2.938	0.479	7.583	
312	15	MOMS	0.348	34.321	0.111	1.847	0.570	6.214	
315	15	LSQ	0.266	41.790	0.206	2.460	0.528	7.651	1.127
			(0.022)	(3.441)	(0.037)	(0.280)	(0.020)	(0.635)	
315	15	MOMCE	0.280	40.000	0.223	2.830	0.498	7.660	
315	15	MOMS	0.307	35.400	0.152	1.793	0.540	6.459	
318	15	LSQ	0.317	39.304	0.146	2.446	0.536	7.039	1.135
			(0.001)	(2.000)	(0.018)	(0.240)	(0.018)	(0.144)	
318	15	MOMCE	0.308	40.000	0.142	2.013	0.549	6.994	
318	15	MOMS	0.305	40.307	0.139	1.773	0.555	6.918	
320	15	LSQ	0.381	39.281	0.134	1.771	0.485	6.883	1.050
			(0.014)	(1.430)	(0.018)	(0.231)	(0.010)	(0.368)	
320	15	MOMCE	0.381	40.000	0.142	2.293	0.476	7.202	
320	15	MOMS	0.383	39.721	0.138	2.229	0.478	7.122	

Standard deviations are noted in parentheses. LSQ, least squares itterative reconvolution analysis; MOMCE, method of moments with Chang-Eisenthal filtering; MOMS, method of moments analysis.

range. The output from the TAC was processed and accumulated in a model 1750 multichannel analyzer (MCA) (Tracor Northern, Middleton, WI). Data was usually collected on a 40- or 20-ns TAC/MCA time range with 1,024 channel resolution. Time ranges and the Ortec nanosecond delays were calibrated with the 81-MHz dye laser pulse repetition rate. The instrument response function was measured by scattering the excitation light from a colloidal suspension of Ludox. The scattered light was filtered through a solar blind filter (Corion Corp., Holliston, MA) before detection. The FWHM of the instrument response function was typically 150 ps.

The intensity of the input light was controlled by a half-wave-plate/polarizer combination at the input of the sample compartment. The excitation intensity was maintained at a level at which the ratio of the rates of "start" to "stop" pulses was always <2% to avoid biasing the data with two-photon events (pulse pileup). Typically, data was collected at 10k counts/s. In addition, fluorescence and response functions were collected at the same count rate to eliminate deconvolution errors caused by changes in the width and shape of the response function due to the count rate dependence of the MCP. In the anisotropy experiments separate response functions were collected for both vertical and horizontal emission components at the corresponding matched count rates.

The Ludox scatterer and fluorescent samples were held in a four-chamber rotating turret on which the polarizer and filters were mounted. The temperature of the sample turret was controlled thermoelectrically with a temperature stability of 0.01°C. The entire system was interfaced to an IBM PC that was used to alternate collection of the sample fluorescence and response functions, automatically match count rates by adjusting the half wave plate attenuator, and control data collection, storage, and transfer of the data from the MCA to an IBM PC floppy disk file. Fluorescence decay and response functions were usually collected in 60-s duration cycles to minimize the effects of drift in the electronics and laser intensity on the measurements. After completion of an experiment, the data was sent to a DEC LSI11/73 computer for analysis.

To fully eliminate the effects of fluctuations in the intensity of the laser during the course of the anisotropy experiments, we collected horizontal and vertical decay components for the same total excitation intensity rather than for equal lengths of time (Fleming and Cross, 1984). This was accomplished by sending a fraction of the excitation beam into an intensity integrator (1P28PMT/amplifier combination) which was interfaced to the IBM PC through an A/D port. The PC then monitored the total intensity and controlled the MCA data acquisition time. A scaling factor to account for optical differences in the collection of these decay components was determined by rotating the excitation polarization 90° and comparing the integrated intensity of the two components. Because the fluorescence is collected in a 90° geometry, the parallel and perpendicular polarization components of the emission should be equal for excitation polarized in the scattering plane.

Magic angle lifetime experiments were analyzed using both the method of moments (Isenberg and Dysan, 1969) with moment index displacement (Isenberg, 1973; Small and Isenberg, 1977) and by iterative reconvolution using a Marquardt nonlinear least square algorithm (Marquardt, 1963). The quality of the fits obtained with the nonlinear least squares fitting procedures were judged by the (reduced) chi-squared value and the randomness of the modified residuals (residuals divided by the square root of the number of counts). Randomness was evalulated by visual inspection of plots of both the residuals and the Poisson-weighted autocorrelation function of the residuals, versus channel number as well as by the "runs test" (time sequence of signs of the residuals; Ameloot and Hendrickx, 1982; Grinvald and Steinberg, 1974). The quality of the method of moments analyses was determined by the agreement between results obtained at different moment displacement values, the lambda-invariance test based on exponential depression, and component incrementation (Isenberg and Small, 1982; Libertini and Small, 1983). In both methods the total fluorescence intensity was assumed to decay as a sum of exponentials. A comparison of the results obtained with these various methods is given in Table 1. For the most part there is good agreement between the methods of analysis. None of the conclusions presented here are influenced by the details of the analysis method.

The anisotropy data were fit using a Marquardt nonlinear least squares search. The horizontal and vertical fluorescence decay curves were simultaneously fit (Fleming and Cross, 1984) using separate horizontal and vertical response functions that were determined at the same count rate as their corresponding fluorescence decay components. The details of the analyses of the anisotropy decays are not relevant to this present discussion and will be presented in another paper (Ruggiero and Hudson, 1989).

RESULTS

The time dependence of the fluorescence of *trans*-parinaric acid in fluid phase lipid bilayers near their phase transition point is described by three exponential components: a short lifetime component with a small amplitude and intermediate and long lifetime components

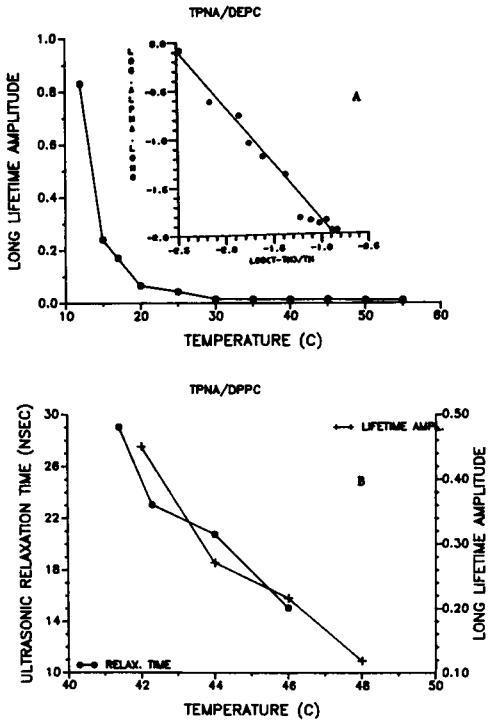

FIGURE 2. The temperature dependence of the amplitude of the long lifetime component of the fluorescence of *trans*-parinaric acid in (*A*) DEPC and (*B*) DPPC bilayer vesicles. The inset in *A* shows the DEPC data plotted on a log (amplitude) vs. log $[(T - T_m)/T_m]$, where T_m = 12°C. The slope of this plot is the critical exponent. (*B*) The variation of the amplitude of the long lifetime component of *trans*-parinaric acid fluorescence (right scale, +) and the ultrasonic relaxation time (left scale, from Mitaku et al., 1982) for DPPC vesicles (T_m = 41°C).

with appreciable amplitudes (Table I). The lifetimes of these components are well separated, especially in DEPC. The amplitude of the long-lived species is an appreciable fraction of the total decay even at temperatures well above T_m. For temperatures below T_m the long lifetime species is the dominant species. These lifetime component amplitudes are not dependent on the probe concentration, method of preparation of the bilayer vesicles or thermal history of the sample. The fluorescence behavior is independent of the emission wavelength. The amplitude of the long-lifetime component is strongly dependent on temperature in the region of the lipid thermal phase transition point (T_m) (Fig. 2); as the temperature is lowered the amplitude of long lifetime component dramatically increases in amplitude.

The inset in Fig. 2 *A* shows the variation of the logarithm of the amplitude of the long-lifetime component as a function of the logarithm of the reduced temperature $(T - T_m)/T_m$. The linearity of this plot is consistent with classical critical exponent behavior. The reasonable degree of conformity of the data to this correlation indicates that the values of the long time component amplitudes are reasonably accurate over almost two orders of magnitude variation.

The lifetime values observed for *trans*-parinaric acid in DEPC for temperatures above T_m are roughly 1, 5, and 10–40 ns; for DPPC this range of values is much compressed (0.6, 1.8, and 5.5 ns). The variation of the value of the longest lifetime with temperature near T_m depends on the particular lipid (Fig. 3). For DEPC there is a sharp drop from ~40 to ~11 ns over a range of ~10°C. In contrast, the long-lifetime value for DPPC bilayers remains fairly constant with temperature.

In simple alkane solvents the emission of *trans*-parinaric acid has been shown by both pulse fluorometry (Ruggiero, 1986) and multifrequency phase fluorometry (Parasassi et al., 1984) to be best described by what is essentially a double exponential decay with temperature-dependent preexponential factors and lifetimes. (Both studies note the presence of a third temperature-independent component with a negligible preexponential factor [<1%] which has been neglected in both analyses.)

The lifetime behavior of *trans*-parinaric acid in DPPC bilayers near the phase transition temperature (T_m = 41.5°C) can be contrasted with its behavior over the same temperature range in *n*-hexadecane solution and DOPC bilayers (T_m = −20°C. *n*-Hexadecane is the alkane analog of the 16-carbon DPPC acyl chains and has been shown by NMR (Brown and Williams, 1985) to closely match the "fluidity" of the hydrocarbon region of the lipid bilayer in the high temperature fluid phase. For

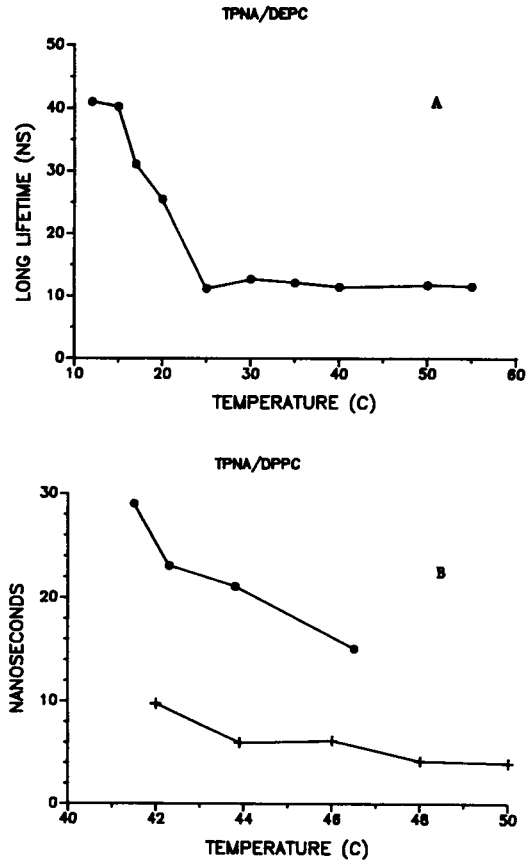

FIGURE 3. (*A*) The temperature variation of the value of the long lifetime component of *trans*-parinaric acid in DEPC vesicles. (*B*) The variation of the lifetime of the long-lived component of *trans*-parinaric acid fluorescence in DPPC vesicles (+). The variation of the ultrasonic relaxation time (from Mitaku et al., 1982) is also shown (●)

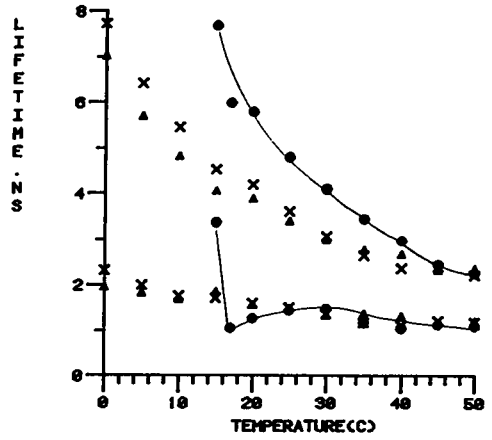

FIGURE 4 Variation with temperature of the values of the intermediate (*upper curves*) and short (*lower curves*) lifetime components of *trans*-parinaric acid in DEPC vesicles (●) superimposed on the lifetime components of *trans*-parinaric acid in DOPC (T_m = −20°C, ×) and for a squalane solution (△) over the same temperature region.

trans-parinaric acid in DPPC vesicles in the 42–50°C temperature range, the values for the three observed lifetime components are ~0.6, 2.5, and 5.5 ns. In both *n*-hexadecane and DOPC over the same temperature region there are only two exponential components with appreciable amplitudes with lifetimes of ~1.0 and 2.8 ns. The two lifetime components observed in hydrocarbon solution correspond most closely with the intermediate and short lifetime components observed for the bilayers. The temperature variation of the intermediate and short lifetime values for *trans*-parinaric acid in DEPC is compared with the two components of the decay observed in DOPC bilayers and squalane solutions in Fig. 4. It appears that at temperatures sufficiently above the phase transition, the bilayer values approach each other and the solution values both in terms of value and temperature dependence.

The variation of the amplitude of the long-lifetime component with excitation wavelength is of particular importance in this study. The data for DEPC and DPPC are shown in Fig. 5. The main point is that at temperatures just above T_m, where the long lifetime component has a major amplitude, this quantity varies by almost a factor of two with change in excitation wavelength. The oscillation observed has the periodicity of the absorption spectrum of parinaric acid with peaks that are red shifted relative to the overall fluorescence excitation spectrum. The corresponding variation in the value of the longest lifetime with excitation wavelength for DEPC is shown in Fig. 6. The constancy of these values demonstrates better than any statistical analysis for a given data set the accuracy of these determinations even when the amplitude of this long lived component is very small.

The time-dependent anisotropy observed for *trans*-parinaric acid in DEPC bilayers at various temperatures is shown in Fig. 7. For low temperatures ($T < T_m$) or very high temperatures ($T \gg T_m$), the anisotropy decays to a constant value; at intermediate temperatures there is a clear rise from a minimum at 5–10 ns to a maximum value at long times. The solid curves drawn through the data are theoretical fits based on a two-environment model (Ludescher et al., 1987). The details of this analysis will be discussed elsewhere (Ruggiero and Hudson, 1989).

The asymptotic value of the anisotropy at long times is related to the (second rank) order parameter, $\langle P_2 \rangle$, of the acyl chain distribution (Heyn, 1979; Jahnig, 1979*a* and *b*; Szabo, 1984; van der Meer et al., 1984; Zannoni, 1981; Zannoni et al., 1983). This limiting value is easily determined from anisotropy experiments because it does not depend appreciably on the details of deconvolution or the detailed time dependence of the anisotropy. A high value for the limiting anisotropy at long times reflects high acyl chain order. A low anisotropy at intermediate times with a rise at longer times is caused by the decreasing contribution of a population with low order having a relatively short fluorescence lifetime. These anisotropy data by themselves demonstrate that there is a correlation between acyl chain order and lifetime with the long-lived species having the higher order. Given the selective

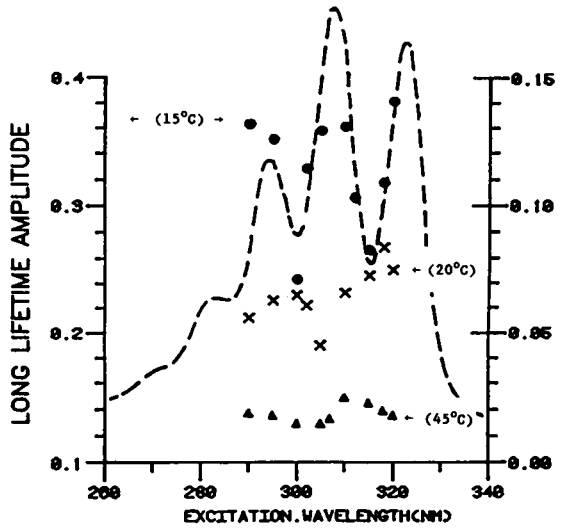

FIGURE 5 The excitation wavelength dependence of the amplitude of the long lifetime component for *trans*-parinaric acid fluorescence in DEPC vesicles at 15°C (●), 20°C (×) and 45°C (△). The 15°C data correspond to the left scale; the higher temperatures correspond to the right scale. A typical absorption spectrum of *trans*-parinaric acid is shown for comparison. Similar behavior is obtained for DPPC vesicles at 46°C.

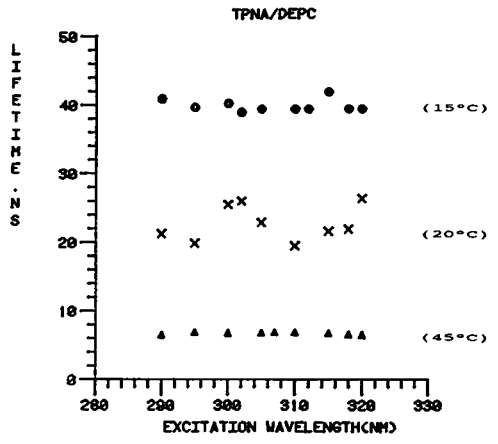

FIGURE 6 Variation of τ_1, the value of the long lifetime, for *trans*-parinaric acid in DEPC vesicles with excitation wavelength at the indicated temperatures. The constancy of these values exemplifies the precision of the lifetime determinations even when (as at 45°C) the amplitude of this component is only 1.7% of the total.

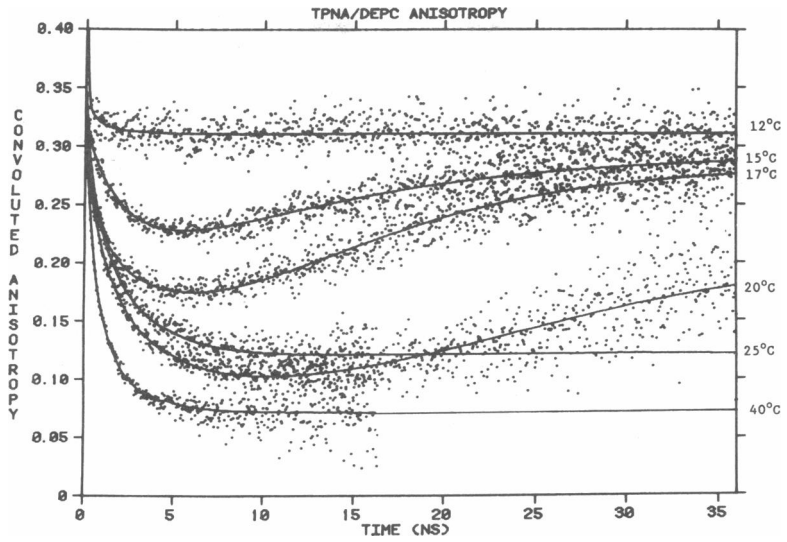

FIGURE 7 Fluorescence anisotropy decay for *trans*-parinaric acid in DEPC vesicles at the indicated temperatures. The solid curves are fits based on a two-environment model (Ludescher et al., 1987). For each environment the anisotropy behavior is given by the form described by Szabo (1984). (For 12 and 40°C only one environment is used in the the fit). The optimized functional form is convoluted with the instrument response function for direct comparison with the data.

excitation data presented above that demonstrate a correlation between fluorescence lifetime and lateral density, it is expected that there will be a selective effect of excitation on the anisotropy behavior. This is illustrated in Fig. 8 for DPPC bilayers vesicles.

DISCUSSION

Trans-parinaric acid has been extensively characterized as a membrane probe (Sklar et al. 1975, 1976, 1977 *a* and *b*; Wolber and Hudson, 1981, 1982; Hudson and Cavalier, 1988). This molecule closely resembles the acyl chains of phospholipids and has a defined depth and orientation in the bilayer. Its hydrophobic nature and negligible quantum yield in water assure that the fluorescence emanates from within the bilayer and not from the surrounding aqueous environment. The spectroscopic and photophysical characteristics of *trans*-parinaric acid are quite different in solid and fluid phase lipids. In low-temperature gel phase lipid, *trans*-parinaric acid has a long average lifetime (30–50 ns), a fluorescence excitation spectrum that is shifted to longer wavelengths by ~2 nm relative to the fluid phase, a high static anisotropy (0.30–0.35) and a time-dependent anisotropy that is essentially constant with time at a high value. In the fluid, liquid crystalline phase, on the other hand, this probe exhibits a much shorter average lifetime (~3.0 ns), a lower static anisotropy (0.10–0.15), and an anisotropy decay that falls rapidly to a nearly constant value much lower than that observed in the solid phase. These properties of *trans*-parinaric acid are understandable in terms of the structure of the bilayer in the solid and fluid phase, and the sensitivity of the excited ^1B_u electronic state of the tetraene chromophore to the polarizability of its environment, a characteristic common to linear conjugated polyenes (Hudson et al., 1982). More specifically, the only solvent interaction that can result in a significant shift in

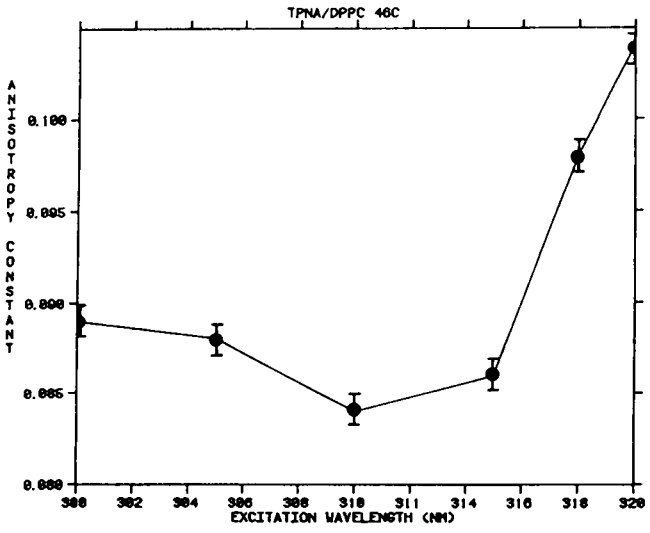

FIGURE 8 Variation of the asymptotic anisotropy of *trans*-parinaric acid in DPPC bilayer vesicles at 46°C with excitation wavelength.

the absorption spectrum of a symmetric linear polyene chromophore is that due to polarizability. For a given chemical composition, the polarizability is proportional to the molecular density. The shift to shorter wavelength in the fluorescence excitation and absorption spectra of parinaric acid in bilayers on going from the higher density solid phase to the lower density fluid phase quantitatively reflects the lower polarizability of the high-temperature fluid phase due to the 3–5% volume expansion associated with the transition (Sklar et al., 1977*b*).

Another feature of the spectroscopy of linear conjugated polyenes that needs to be kept in mind to understand their photophysical behavior is that the absorption spectrum is dominated by a strong transition to the second excited singlet electronic state (the 1^1B_u state); the fluorescence originates from the first excited singlet electronic state (the 2^1A_g state). The lowest excited 2^1A_g state results in a forbidden electronic transition from the ground electronic state (the 1^1A_g state). As a result, this transition does not make a significant contribution to the absorption spectrum so that the observed absorption (or fluorescence excitation) spectrum exhibits shifts that are not reflected in the emission spectrum. The emission spectrum is, in fact, essentially independent of environment. Because of this state ordering, the fluorescence lifetime of parinaric acid is much longer than would be expected on the basis of the intense absorption spectrum. The radiative lifetime for parinaric acid is several hundred nanoseconds; the observed lifetime of 1–40 ns reflects the importance of the radiationless processes competing with emission. This radiationless decay rate has a significant temperature dependence in both solid and fluid phase lipid bilayers and in solution. Because of this the lifetime of parinaric acid in bilayers decreases with increasing temperature and is higher at the transition temperature for lipids with a low T_m (Sklar et al., 1977*b*).

The observation of a long lifetime component in fluid phase lipid bilayers with an amplitude that is strongly dependent on the relative distance from the phase transition point (Fig. 2) suggests that a *trans*-parinaric species may exist near the transition point in an environment that is structurally different (more "solidlike") than the bulk fluid phase lipid. The nature of the probe environment giving rise to a long lifetime is confirmed by the behavior of the amplitude of this component as a function of excitation wavelength. The proposed solidlike environment, because of its higher density (polarizability), should result in an excitation spectrum that is shifted to longer wavelengths relative to the overall fluorescence excitation spectrum. This is indeed observed. Fig. 5 shows the amplitude of the long lifetime component of *trans*-parinaric acid in DEPC vesicles plotted as a function of excitation wavelength overlaid on the absorption spectrum of *trans*-parinaric acid obtained in hexadecane solution. *Trans*-parinaric acid in solution (and for bilayers at temperatures far above T_m) does not exhibit this excitation wavelength dependence of the amplitudes. (Recall that under these circumstances parinaric acid exhibits two decay components corresponding roughly to the intermediate and short lifetimes observed in bilayers near their transition temperature.) The parinaric acid species present in bilayers for T slightly greater than T_m that gives rise to a long fluorescence lifetime therefore has two properties characteristic of a solid lipid environment: the long lifetime itself and the red-shifted excitation spectrum reflecting a higher local density.

A model has been constructed that accounts for the photophysical and spectroscopic properties of parinaric acid in solution (Ruggiero, 1986; Ruggiero and Hudson, manuscript in preparation). By extension, this model can be applied to the behavior observed for this probe in bilayers. The essence of this model is that in fluid solution, and in fluid phase bilayers, parinaric acid undergoes an excited state interconversion process between species with distinct fluorescence lifetimes but having essentially the same emission spectra. The lack of any excitation wavelength dependence to the decay amplitudes for the solution case is characteristic of an excited state relaxation process. The kinetic treatment of this model follows standard procedures (Demas, 1983). The result is that the decay constants reflect both the intrinsic decay rates and the interchange rates between species. It is proposed that the interchange rate is temperature dependent such that at high temperature dynamic averaging will set in resulting in a single decay time that is an average of that for each species. This behavior is demonstrated for squalane in Fig. 4.

Bilayers at temperatures near T_m differ from the solution case in that they provide an additional solidlike environment for the probe in which the probe lifetime is long compared with that of the fluid environment. The values of the short and intermediate lifetimes for *trans*-parinaric acid in DEPC and DPPC bilayers, and their temperature dependence, are very similiar to the behavior of *trans*-parinaric acid in DOPC ($T_m = -20°C$) and squalane (a low melting saturated hydrocarbon) over the same temperature region (Fig. 4). We are therefore led to the conclusion that the behavior of parinaric acid in fluid phase bilayers is similar to that in solution giving rise to two apparent decay components in the 1–8 ns range. The slight differences between the lifetimes of *trans*-parinaric acid in DEPC near the transition point and the solution and DOPC cases reflects the fact that the decay parameters in DEPC are kinetically coupled to the solid phase due to the finite rate of formation and dissipation of the solidlike domains. In other words, the probe spends some of its time in the solid regions and this is reflected in its

decay time. Above 30° the amplitude of the solidlike domains for DEPC bilayers becomes very small and the lifetime values approach those observed in solution. The two DOPC lifetime values are quite close to those observed in solution throughout this temperature range because this lipid has a very low T_m.

The observation of component selection by variation of the excitation wavelength (Table 1 and Fig. 5) suggests that these solidlike domains have a characteristic lifetime that is long compared with the fluorescence lifetime of the probe (several nanoseconds). A comparison of the temperature dependence of the amplitude of long lifetime species found in DPPC vesicles with the corresponding temperature dependence of the ultrasonic relaxation times measured by Mitaku and Date (1982) for this same lipid is shown in Fig. 2 *B*. The ultrasonic data reflect the relaxation time of fluctuations in bulk density presumably through changes in lateral compressibility. A strong correlation is observed between the ultrasonic data and the amplitude of the long lifetime fluorescence component. As mentioned earlier, these fluctuations are believed to be associated with the formation and existence of solidlike clusters of lipid in the fluid phase bilayer. When the transition temperature is approached from above the relaxation time of these fluctuations increases rapidly and so does the probability of finding a parinaric acid molecule in a solidlike environment. The much shorter lifetime (~5 ns) of the probe species in the solid DPPC domains compared with the 10–30 ns ultrasonic relaxation time suggests that the fluorescence decay time is not modulated by the long-range structural fluctuations detected in the ultrasonic measurements. This is confirmed by the fact that, despite the rapid variation of the density fluctuation correlation time in this temperature region, the value of the long lifetime is not a strong function of temperature. This fact demonstrates that the probe environment is static on the fluorescence time scale in this case.

In contrast, the lifetime of the long-lived component in DEPC bilayers at temperatures just above T_m (12°) (Fig. 3) is much longer then is the case for DPPC at 50°. This increase in the probe lifetime reflects the general temperature dependence of the radiationless decay rate for linear polyenes. In the DEPC case the probe lifetime is comparable with the persistence time for the density fluctuations. The rapid variation of the value of this long lifetime from 40 to 10 ns in the temperature region just a few degrees above T_m is consistent with the significance of the density fluctuation rate to the observed decay time, i.e., the finite lifetime of the solid phase environment contributes to the decay of the fluorescence in this case.

The solidlike nature of the long-lifetime probe environment is perhaps most convincingly demonstrated by the anisotropy behavior observed in DEPC (Fig. 7). The large difference between the lifetimes of the solid and fluid species in this case causes the solidlike environment with its longer lifetime and higher anisotropy to dominate the decay at long times. This results in the observed upward curvature. This type of decay behavior is the signature of a system with heterogeneity in which there is a correlation between fluorescence lifetime and reorientational motion (Ludescher et al., 1987). The anisotropy decay data is well fit by a model that includes two probe environments with distinct anisotropy behavior. Specifically, the short and intermediate lifetime components are associated with a long rotational correlation time and a low value for the limiting anisotropy; the long lifetime component is associated with a short rotational correlation time and a relatively high anisotropy constant. This last property is characteristic of an ordered environment. It is not possible to fit this data without assuming rotational heterogeneity. The use of this type of anisotropy model with the DPPC data also resulted in good fits to the data by using the same type of association between lifetime components and rotational correlation times. In this case however, large uncertainties often resulted in the estimated parameters. This is because the small difference between the component lifetimes of *trans*-parinaric acid in DPPC does not result in the observation of distinct upward curvature in the anisotropy decay. Because the signal-to-noise ratio of the measurement is decreasing with time, the resolution of the anisotropy behavior of the different rotational species is much more difficult for DPPC than for DEPC and does not permit the long time behavior to be cleanly resolved. A detailed discussion of the parameters extracted from the anisotropy results will be given elsewhere (Ruggiero and Hudson, 1989).

This observation of anisotropy behavior exhibiting upward curvature is of fundamental importance in this study because it connects the fluorescence lifetime decay behavior and the motional behavior of the fluorophores in the sample without any assumptions as to the precise number of exponential components that must be used to describe the data. It has been shown (Ludescher et al., 1987) that the only model resulting in anisotropy decay behavior of the type shown in Fig. 7 is one in which long-lived species have a higher anisotropy than other shorter-lived species. The essence of the argument is that other models (such as anisotropic rotational diffusion of a homogeneous population of species) that may give rise to anisotropy behavior that rises in time require noncollinear absorption and emission dipoles. This can be eliminated as a possibility in this case because of the high initial value of the anisotropy (~0.35). Thus, the anisotropy behavior directly demonstrates the presence of long-lifetime species with restricted angular range, two features characteristic of gel phase lipids.

This analysis of the anisotropy decay data is interre-

lated with the analysis of the fluorescence decay data in terms of a finite number of exponential components. It has been proposed (James and Ware, 1985, 1986) that data that appears to be described in terms of a sum of exponential components may, in fact, arise from a continuous distribution of decay times. This is certainly a physically reasonable possibility in many circumstances including lipid bilayers. In the present case, however, the anisotropy decays and the excitation wavelength behavior demonstrate that even if the population of fluorophores is better represented by a continuous distribution, there must be a correlation between the long-lifetime tail of this distribution, the absorption spectrum of these species, and their reorientational amplitude. It is convenient to use a discrete population analysis of these observations and, because this analysis is adequate to describe the data, it is not clear that a more complex analysis is warranted.

The variation of the limiting anisotropy with excitation wavelength for DPPC bilayer vesicles shown in Fig. 8 demonstrates the expected connection between the absorption spectrum of the probe in a solidlike environment and its motional freedom. These diverse experimental observations for two distinct bilayers are mutually interrelated and internally consistent. The differences observed for DPPC and DEPC (as well as DOPC) bilayers are related to the differences in T_m and the established temperature dependence of the photophysical properties of *trans*-parinaric acid.

The temperature variation of the amplitude of the long-lifetime component of the fluorescence follows that expected for critical behavior. The value of the critical exponent obtained from this data (Fig. 2) is 1.10 ± 0.10. This value is very similar to the classical Landau value of 1.0 which seems to be adequate to describe the temperature variation of ultrasonic data (Mitaku et al., 1983). It is also close to the value of 1.05 deduced in the theoretical treatment of Mouritsen and Zuckermann (1985). A discussion of precise values is not warranted at this time pending refinement of the precision of the fluorescence data. The degree of agreement of the form of the temperature variation of the fluorescence data with expectations based on a critical model supports the basic interpretation presented here.

CONCLUSIONS

The examination of the time-resolved fluorescence properties of *trans*-parinaric acid in liquid crystalline phase DPPC and DEPC lipid bilayers reveals the existence of metastable regions of ordered solidlike lipids in the phase transition region with a temperature dependence similar to that observed for critical phenomena. The association of the fluorescence decay behavior with the transient formation of lipid structural domains is based on the sensitivity of the *trans*-parinaric acid excited state photophysics to the local environment, particularly the polarizability of its surroundings. These physical properties of *trans*-parinaric acid enable the fluorescence anisotropy decay of this probe to be resolved into contributions from two rotationally distinct environments that can be characterized by their long-range orientational order and acyl chain dynamics and correspond to probe molecules in the bulk fluid phase bilayer and solidlike lipid clusters.

The liquid crystalline phase lipid bilayer near the phase transition point can be viewed as a "flickering" structure with the transient alignment and packing of the lipid hydrocarbon chains trapping the probe species in a solidlike environment and then dissipating to reform the fluid domain on the fluorescence timescale. The relaxation time of these structural fluctuations is much shorter than the time required to establish lateral spatial equilibration of the probe. This picture is consistent with the theoretical work of Mouritsen and Zuckermann (1985) and the ultrasonic velocity measurements of Mitaku et al. (1983). Furthermore, it provides a microscopic explanation for the "continuous" nature of the first order phase transition observed experimentally for certain macroscopic physical properties of the bilayer such as the passive permeability (Papahadjopoulos et al. 1973; Doniach, 1978) and specific heat (Hatta et al., 1983, 1984).

We wish to thank John Nagle for helpful comments.

This work was supported by National Institutes of Health grant GM26536.

Received for publication 28 October 1988.

REFERENCES

Ameloot, A., and H. Hendrickx. 1982. Criteria for model evaluation in the case of deconvolution calculations. *J. Chem. Phys.* 76:4419–4432.

Barrow, D., and B. Lentz. 1985. Membrane structural domains: resolution limits using diphenylhexatriene fluorescence decay. *Biophys. J.* 48:221–234.

Berde, C. B., H. C. Andersen, and B. Hudson. 1980. A theory of the effects of headgroup structure and acyl chain unsaturation on the chain melting transition of neutral aqueous phospholipid dispersions. *Biochemistry.* 19:4279–4293.

Brown, M. F., and A. A. Williams. 1985. Membrane NMR: a dynamic research area. *J. Biochem. Biophys. Methods.* 11:71–81.

Busico, V., and M. Vacatello. 1983. Lipid bilayers in the 'fluid' state: computer simulation and comparison with model compounds. *Mol. Cryst. Liq. Cryst.* 97:195–207.

de Gennes, P. G. 1972. Short range order effects in the isotropic phase of nematics and cholesterics. *Mol. Cryst. Liq. Cryst.* 12:193–214.

de Gennes, P. G. 1974. The Physics of Liquid Crystals. Oxford University Press, Oxford.

Demas, A. 1983. Excited State Lifetime Measurements. Academic Press, New York.

Doniach, S. 1978. Thermodynamic fluctuations in phospholipid bilayers. *J. Chem. Phys.* 68:4912–4916.

Fleming, G. R. 1986. Chemical Applications of Ultrafast Spectroscopy. Oxford University Press, New York.

Fleming, G. R. and A. J. Cross. 1984. Analysis of time-resolved fluorescence anisotropy decays. *Biophys. J.* 46:45–56.

Grinvald A., and I. Z. Steinberg. 1974. On the analysis of fluorescence decay kinetics by the method of least-squares. *Anal. Biochem.* 59:583–598.

Hatta, I., D. Suzuki, and S. Imaizumi. 1983. Pseudo-critical heat capacity of single lipid bilayers. *J. Phys. Soc. Jpn.* 52:2790–2797.

Hatta, I., S. Imaizumi, and Y. Akutsu. 1984. Evidence for weak first-order nature of lipid bilayer phase transition from the analysis of pseudo-critical specific heat. *J. Phys. Soc. Jpn.* 53:882–888.

Heyn, M. P. 1979. Determination of lipid order parameters and rotational correlation times from fluorescence depolarization experiments. *FEBS (Fed. Eur. Biochem. Soc) Lett.* 108:359–364.

Hudson, B., and S. Cavalier. 1988. Studies of membrane dynamics and lipid-protein interactions with parinaric acid. *In* Spectroscopic Membrane Probes. Vol. 1. L. Loew, editor. CRC Press, Inc., Boca Raton, FL 43–62.

Hudson, B., B. E. Kohler, and K. Schulten. 1982. Linear Polyene Electronic Structure and Potential Surfaces. Excited States 6. E. C. Lim, editor. Academic Press, New York. 1–95.

Isenberg, I. 1973. On the theory of fluorescence decay experiments. I. Nonrandom distortions. *J. Chem. Phys.* 59:5696–5707.

Isenberg, I., and R. D. Dysan. 1969. The analysis of fluorescence decay by a method of moments. *Biophys. J.* 9:1337–1350.

Isenberg, I., and E. W. Small. 1982. Exponential depression as a test of estimated decay parameters. *J. Chem. Phys.* 77:2799–2805.

Jacobs, R. E., B. Hudson, and H. C. Andersen. 1975. A theory of the chain melting phase transition of aqueous phospholipid dispersions. *Proc. Natl. Acad. Sci. USA.* 72:3993–3997.

Jacobs, R. E., B. Hudson, and H. C. Andersen. 1977. A theory of phase transitions and phase diagrams for one- and two-component phospholipid bilayers. *Biochemistry.* 16:4349–4359.

Jahnig, F. 1979*a*. Molecular theory of lipid membrane order. *J. Chem. Phys.* 70:3279–3290.

Jahnig, F. 1979*b*. Structural order of lipids and proteins in membranes: evaluation of fluorescence anisotropy data. *Proc. Natl. Acad. Sci. USA.* 76:6361–6365.

Jahnig, F. 1981*a*. Critical effects from lipid-protein interaction in membranes. I. Theoretical description. *Biophys. J.* 36:329–345.

Jahnig, F. 1981*b*. Critical effects from lipid-protein interaction in membranes. II. Interpretation of experimental results. *Biophys. J.* 36:347–357.

Jahnig, F. 1981*c*. The ordered-fluid transition in lipid bilayers. *Mol. Cryst. Liq. Cryst.* 63:157–170.

James, D. R., and W. R. Ware. 1985. A fallacy in the interpretation of fluorescence decay parameters. *Chem. Phys. Lett.* 120:455–459.

James, D. R., and W. R. Ware. 1986. Recovery of underlying distributions or lifetimes from fluorescence decay data. *Chem. Phys. Lett.* 126:7–11.

Kanehisa, M. I., and T. Y. Tsong. 1978. Cluster model of lipid phase transitions with application to passive permeation of molecules and structure relaxations in lipid bilayers. *J. Am. Chem. Soc.* 100:424–432.

Karnovski, M. J., A. M. Kleinfeld, R. L. Hoover, E. A. Dawidowicz, D. E. McIntyre, E. A. Salzman, and R. D. Klausner. 1982. Lipid domains in membranes. *Ann. NY Acad. Sci.* 401:61–75.

Klausner, R. D., A. M. Kleinfeld, R. L. Hoover, and M. J. Karnovsky. 1980. Lipid domains in membranes. *J. Biol. Chem.* 255:1286–1295.

Knoll, W., G. Schmidt, E. Sackmann, and K. Ibel. 1983. Critical demixing in fluid bilayers of phospholipid mixtures. A neutron diffraction study. *J. Chem. Phys.* 79:3439–3442.

Kox, A. J., J. P. J. Michels, and F. W. Wiegel. 1980. Simulation of a lipid monolayer using molecular dynamics. *Nature (Lond.).* 287:317–319.

Kremer, J., M. Esker, C. Pathmamanoharan, and P. Wiersema. 1977. Vesicles of variable diameter prepared by a modified injection method. *Biochemistry.* 16:3932–3935.

Lee, A. G. 1977. Lipid phase transitions and phase diagrams. I. Lipid phase transitions. *Biochim. Biophys. Acta.* 472:237–281.

Libertini, L., and E. Small. 1983. Resolution of closely spaced fluorescence decays: the luminescence background of the RCA 8850 photomultiplier and other sources of error. *Rev. Sci. Instrum.* 54:1458–1466.

Ludescher, R. D., L. Peting, S. Hudson, and B. Hudson. 1987. Time-resolved fluorescence anisotropy for systems with lifetime and dynamic heterogeneity. *Biophys. Chem.* 28:59–75.

Marcelja, S. 1976. Chain ordering in liquid crystals. II. Structure of bilayer membranes. *Biochim. Biophys. Acta.* 367:165–176.

Marcelja, S., and J. Wolfe. 1979. Properties of bilayer membranes in the phase transition or phase separation region. *Biochim. Biophys. Acta.* 557:24–31.

Marquardt, D. W. 1963. An algorithm for least-squares estimation of nonlinear parameters. *J. Soc. Indust. Appl. Math.* 11:431–467.

McCammon, J. A., and J. M. Deutch. 1975. Semiempirical models for biomembrane phase transitions and phase separations. *J. Am. Chem. Soc.* 97:6675–6681.

Mitaku, S., and T. Date. 1982. Anomalies of nanosecond ultrasonic relaxation in the lipid bilayer transition. *Biochim. Biophys. Acta.* 688:411–421.

Mitaku, S., and K. Okano. 1981. Ultrasonic measurements of two-component lipid bilayer suspensions. *Biophys. Chem.* 14:147–158.

Mitaku, S., A. Ikegami, and A. Sakanishi. 1978. Ultrasonic studies of lipid bilayer. Phase transition on synthetic phosphatidylcholine liposomes. *Biophys. Chem.* 8:295–304.

Mitaku, S., T. Jippo, and R. Kataoka. 1983. Thermodynamic properties of the lipid bilayer transition. *Biophys. J.* 42:137–144.

Mouritsen, O., and M. Zuckermann. 1985. Softening of lipid bilayers. *Eur. Biophys. J.* 12:75–86.

Mouritsen, O., A. Boothroyd, R. Harris, N. Jan, T. Lookman, L. MacDonald, D Pink, and M. Zuckermann. 1983. Computer simulations of the main gel-fluid transition of lipid bilayers. *J. Chem. Phys.* 79:2027–2041.

Nagle, J. F. 1973*a*. Theory of biomembrane phase transitions. *J. Chem. Phys.* 58:252–264.

Nagle, J. F. 1973*b*. Lipid bilayer phase transition: density measurements and theory. *Proc. Natl. Acad. Sci. USA.* 70:3443–3444.

Nagle, J. F. 1976. Theory of lipid monolayer and bilayer phase transitions: effect of headgroup interactions. *J. Membr. Biol.* 27:233–250.

Nagle, J. F. 1980. Theory of the main lipid bilayer phase transition. *Annu. Rev. Phys. Chem.* 31:157–195.

Nagle, J. F., and H. L. Scott. 1978. Lateral compressibility of lipid mono- and bilayers. Theory of membrane permeability. *Biochim. Biophys. Acta.* 513:236–243.

Nagle, J. F., and D. A. Wilkinson. 1978. Lecithin bilayers: density measurements and molecular interactions. *Biophys. J.* 23:159–175.

Northrup, S. H., and M. S. Curvin. 1985. Molecular dynamics simulation of disorder transitions in lipid monolayers. *J. Phys. Chem.* 89:4707–4713.

Owicki, J. C., M. W. Springgate, and H. M. McConnell. 1978. Theoretical study of protein-lipid interaction in bilayer membranes. *Proc. Natl. Acad. Sci. USA.* 75:1616–1619.

Papahadjopoulos, D., K. Jacobson, S. Nir, and T. Isac. 1973. Phase transitions in phospholipid vesicles. *Biochim. Biophys. Acta.* 311:330–348.

Parasassi, T., F. Conti, and E. Gratton. 1984. Study of heterogenous emission of parinaric acid isomers using multifrequency phase fluorometry. *Biochemistry.* 23:5660–5670.

Philips, D. 1985. Time-correlated single photon counting. Academic Press, New York.

Priestley, E. B., P. Wojtowicz, and P. Sheng. 1975. Introduction to Liquid Crystals. Academic Press, New York.

Ruggiero, A. J. 1986. Time-resolved fluorescence studies of pretransitional phenomena in phospholipid bilayers. Ph.D. thesis. University of Oregon, Eugene, OR.

Ruggiero, A. J., and B. S. Hudson. 1989. Analysis of the anisotropy decay of *trans*-parinaric acid in lipid bilayers. *Biophys. J.* 55:1125–1135.

Sakinishi, A., S. Mitaku, and A. Ikegami. 1979. Stabilizing effect of cholesterol on phosphatidylcholine vesicles observed by ultrasonic velocity measurement. *Biochemistry.* 18:2636–2642.

Schindler, H., and J. Seelig. 1975. Deuterium order parameters in relation to thermodynamic properties of a phospholipid bilayer. A statistical mechanical interpretation. *Biochemistry.* 14:2283–2287.

Schroder, H. 1977. Aggregation of proteins in membranes. An example of fluctuation-induced interactions in liquid crystals. *J. Chem. Phys.* 67:1617–1619.

Sklar, L., B. Hudson, and R. Simoni. 1975. Conjugated polyene fatty acids as membrane probes: preliminary characterization. *Proc. Natl. Acad. Sci. USA.* 72:1649–1653.

Sklar, L., B. Hudson, and R. Simoni. 1976. Conjugated polyene fatty acids as fluorescent membrane probes: model system studies. *J. Supramol. Struct.* 4:449–465.

Sklar, L., B. Hudson, and R. Simoni. 1977*a*. Conjugated polyene fatty acids as fluorescent probes: spectroscopic characterization. *Biochemistry.* 16:813–819.

Sklar, L., B. Hudson, and R. Simoni. 1977*b*. Conjugated polyene fatty acids as fluorescent probes: synthetic phospholipid membrane studies. *Biochemistry.* 16:819–828.

Small, E. W., and I. Isenberg. 1977. On moment index displacement. *J. Chem. Phys.* 66:3347–3351.

Stinson, T., III, and J. Litster. 1970. Pretransitional phenomena in the isotropic phase of a nematic liquid crystal. *Phys. Rev. Lett.* 25:503–508.

Szabo, A. 1984. Theory of fluorescence depolarization in macromolecules and membranes. *J. Chem. Phys.* 81:150–167.

van der Meer, W., H. Pottel, W. Herreman, M. Ameloot, and H. Hendrickx. 1984. Effects of orientational order on the decay of the fluorescence anisotropy in membrane suspensions. *Biophys. J.* 46:515–523.

van der Ploeg, P., and J. C. Berendsen. 1982. Molecular dynamics simulation of a bilayer membrane. *J. Chem. Phys.* 76:3271–3276.

van der Ploeg, P., and J. C. Berendsen. 1983. Molecular dynamics of a bilayer membrane. *Mol. Phys.* 49:233–248.

Williamson, H. W., C. G. Morgan, S. Fuller, and B. Hudson. 1983. Melittin induces fusion of phospholipid vesicles. *Biochim. Biophys. Acta.* 732:668–674.

Wojtowicz, P. 1975. Introduction to Liquid Crystals. E. B. Priestly, P. J. Wojtowicz, and P. Sheng, editors. Academic Press, New York.

Wolber, P. K., 1980. A fluorometric study of the structure and acyl chain dynamics of pure phophatidylcholine vesicles, and vesicles containing cholesterol or the M13 coat protein. Ph.D. thesis. Stanford University, Palo Alto, CA.

Wolber, P. K., and B. Hudson. 1981. Fluorescence lifetime and time resolved polarization anisotropy studies of acyl chain order and dynamics in lipid bilayers. *Biochemistry.* 20:2800–2810.

Wolber, P. K., and B. S. Hudson. 1982. Bilayer acyl chain dynamics and lipid-protein interaction. *Biophys. J.* 37:253–262.

Zannoni, C. 1981. A theory of fluorescence depolarization in membranes. *Mol. Phys.* 42:1303–1320.

Zannoni, C., A. Arcioni, and P. Cavatorta. 1983. Fluorescence depolarization in liquid crystals and membrane bilayers. *Chem. Phys. Lipids.* 32:179–250.

Zuckermann, M., and D. Pink. 1980. The correlation length and lateral compressibility of phospholipid bilayers in the presence of thermodynamic density fluctuations. *J. Chem. Phys.* 73:2919–2926.